UAV-aided Secure NOMA Transmission via Trajectory and Resource Optimization

Yanxin Li[†], Wei Wang[†], Mingqian Liu[⋆], Nan Zhao[†], Xu Jiang[†], Yunfei Chen[‡], and Xianbin Wang[II]
[†]School of Information and Communication Engineering, Dalian University of Technology, Dalian, Liaoning, P. R. China
[⋆]State Key Laboratory of Integrated Service Networks, Xidian University, Xi'an, P. R. China
[‡]School of Engineering, University of Warwick, Coventry CV4 7AL, U.K.
[II]Department of Electrical and Computer Engineering, Western University, London, ON N6A 5B9, Canada

2021 13th International Conference on Wireless Communications and Signal Processing (WCSP) | 978-1-6654-0785-4/21/$31.00 ©2021 IEEE | DOI: 10.1109/WCSP52459.2021.9613552

***Abstract*—The application of NOMA in UAV networks is an effective solution for communications. However, the security risk becomes more serious with the LoS channels and higher transmit power for weaker users in NOMA-UAV networks. In this paper, a UAV-assisted NOMA transmission scheme is proposed to achieve secure downlink transmission via artificial jamming, where a UAV flies straightly to serve multiple ground users in the presence of a passive eavesdropper. Only the closest users to the UAV can be connected in each time slot to achieve high LoS probability. To balance the security and transmission performance, the tradeoff between the jamming power and the sum rate is investigated by jointly optimizing the power allocation, the user scheduling and the UAV trajectory. To address the problem, we first decompose the problem into two subproblems of power allocation and trajectory optimization. Then, they are transformed into convex ones for an iterative algorithm via the first-order Taylor expansion. Finally, simulation results are presented to show the effectiveness of the proposed scheme.**

***Index Terms*—Beamforming optimization, non-orthogonal multiple access, physical layer security, power allocation, unmanned aerial vehicle.**

I. Introduction

In recent years, unmanned aerial vehicle (UAV) systems have been widely utilized in different applications, including precision agriculture, forest fire monitoring and search and rescue communications [1]. Due to the advantages of the high mobility and quality of line-of-sight (LoS) air-to-ground links, UAV-assisted wireless networks are developing rapidly [2]. To reduce the number of UAV base stations (BSs) that provide wireless coverage, Lyu *et al*. proposed a novel method of UAV placement in [3], where the UAVs are placed sequentially along a spiral path towards the center until all the ground users are covered. To improve the performance of UAV-assisted terrestrial cellular networks, Wu *et al*. proposed a scheme in [4] to offload terrestrial users from BS to UAV clusters, considering the energy state and cellular load.

On the other hand, non-orthogonal multiple access (NOMA) shares the same resource among multiple users, which can effectively enhance the network capacity and spectrum efficiency [5]. Due to the superiority of NOMA, many research works have been conducted on its applications [6], [7]. In [6], Chen *et al*. proposed a low-complexity sequential user pairing algorithm based on the NOMA precoding algorithm in a MISO-NOMA downlink scenario. Wu *et al*. implemented the BS-user communication with the help of a set of relays in NOMA networks, and a power allocation problem is proposed to maximize the throughput [7].

When the number of NOMA users is large, we can reduce the latency by dividing them into different orthogonal groups and utilize the mobility of UAVs [8], [9]. The applications of NOMA in UAV networks have attracted attentions [10], [11]. In [10], both the UAV trajectory and resource allocation were optimized by Zhao *et al*. to maximize the sum rate. Budhiraja *et al*. minimized the energy efficiency of communication in terms of power and trajectory in the UAV networks [11]. However, the high quality of LoS links makes the transmitted information more susceptible to eavesdropping. [12], [13]. In [12], Wang *et al*. considered UAV relays to secure the wireless communications. Cheng *et al*. jointly optimized the UAV trajectory and the scheduling to guarantee the security in [13], via caching the information for other users.

Considering the LoS channels in NOMA-UAV networks, there is a high risk of being eavesdropped [14], and many studies have been done to guarantee the security of NOMA-UAV networks [15], [16]. In [15], Wang *et al*. optimized the achievable minimum secrecy rate of users served by UAV to satisfy the heterogeneous service requirements in downlink multi-user NOMA transmission. Sun *et al*. used the directional modulation and adaptive genetic simulated annealing algorithm in [16] to improve the security of NOMA-UAV networks in the millimeter wave framework.

Inspired by the above research, in this paper, we propose an artificial jamming aided NOMA-UAV scheme to guarantee the secure transmission first. Then we use Taylor expansion to approximate it as a convex one.

II. System Model

Consider a downlink NOMA-UAV network, where the UAV flies along a straight trajectory to transmit data to K ground single-antenna users. The flight time T can be divided

The work was supported by the National Key R&D Program of China under Grant 2020YFB1807002. Xu Jiang is the corresponding author (jiang_xu@dlut.edu.cn).

978-1-6654-0785-4/21/$31.00 ©2021 IEEE

into N time slots, and the length of each slot is denoted by $\delta_t = \frac{T}{N}$. Assume that δ_t is short enough so that the location of UAV is fixed in each time slot. Define the kth user as U_k, $k=1,2,...,K$, with its location $\mathbf{x}_k=(x_k,y_k)$. Similarly, the coordinates of the UAV in the nth time slot can be denoted as $\mathbf{q}[n]=(x[n],y[n])$. Specifically, the starting and ending points of the UAV are $\mathbf{q}[1]=\mathbf{a}$ and $\mathbf{q}[N]=\mathbf{b}$, respectively. The distance between the UAV and U_k in the nth time slot can be expressed as $d_k[n]=\sqrt{\|\mathbf{q}[n]-\mathbf{x}_k\|^2+H^2}, \forall k,n$. where H is the flight height of the UAV.

The UAV cannot access all the users via NOMA in a single time slot since accessing too many users simultaneously can lead to high complexity, non-line-of-sight (NLoS) channels, and SIC errors. Thus, we assume that the closest C users are chosen to connect with the UAV in each time slot to guarantee the quality of service.

Define $\mathcal{U}[n]=\{u_{1n},u_{2n},...,u_{in},...,u_{Cn}\}$ as the set of C users that are connected with the UAV in the nth time slot, where the users in $\mathcal{U}[n]$ are sorted in the ascending order of distance from the UAV. Define $d_{u_{in}}[n]$ as the distance between the UAV and u_{in}, and the distance relationship between the UAV and the accessed users in the nth time slot can be denoted as $d_{u_{1n}}[n]\leq d_{u_{2n}}[n]\leq ...\leq d_{u_{in}}[n]\leq \ ...\ \leq d_{u_{Cn}}[n]$. The channels between the UAV and connected users can are assumed to be LoS.

Nevertheless, the high-quality LoS channels of UAV are also directly exposed to eavesdroppers. To flight against the potential eavesdropping, artificial jamming is generated by the UAV together with the desired signals. The UAV's transmitted signal in the nth time slot can be expressed as

$$x_{u_{in}}[n]=\sum\nolimits_{i=1}^{C}\sqrt{p_{u_{in}}[n]}s_{u_{in}}[n]+\sqrt{P_{jam}[n]}s_{jam}[n], \quad (1)$$

where $p_{u_{in}}[n]$ is the transmit power for u_{in}, $s_{u_{in}}[n]$ is the transmitted information of u_{in} with $\mathbb{E}\left\{|s_{u_{in}}[n]|^2\right\}=1$, and $s_{jam}[n]$ is the artificial jamming with the transmit power $P_{jam}[n]$. $p_{u_{in}}[n]$ and $P_{jam}[n]$ satisfy

$$\sum\nolimits_{i=1}^{C} p_{u_{in}}[n]+P_{jam}[n]\leq P_{sum}, i=1,...,C, \quad (2)$$

where P_{sum} is the transmit power constraint of UAV. Since the UAV sends a mixture of information and jamming, the received signal at u_{in} is

$$y_{u_{in}}[n]=h_{u_{in}}[n]\left(\sum_{j=1}^{C}\sqrt{p_{u_{jn}}[n]}s_{u_{jn}}[n]+\sqrt{P_{jam}[n]}s_{jam}[n]\right)+z_{u_{in}}, \quad (3)$$

where $z_{u_{in}}\sim\mathcal{CN}(0,\sigma^2)$ is the additive white Gaussian noise (AWGN) at u_{in} with zero mean and variance σ^2. $h_{u_{in}}[n]$ represents the LoS channel coefficient from the UAV to u_{in} in the nth time slot as $h_{u_{in}}[n]=\sqrt{\rho d_{u_{in}}^{-\alpha}[n]}$, where ρ is the parameter of channel gain at the reference distance 1 m, and the path-loss exponent $\alpha=2$.

According to NOMA, the decoding order can be determined according to the distance between the connected users and the UAV in each time slot, i.e., the users farther away from the UAV are decoded first. Thus, in the nth time slot, the transmit power of the connected users should satisfy

$$0\leq p_{u_{1n}}[n]\leq ...\leq p_{u_{in}}[n]\leq ...\leq p_{u_{Cn}}[n]\leq P_{jam}[n]. \quad (4)$$

Since $P_{jam}[n]$ is the highest, the jamming signal is first decoded, and the low-power legitimate signals can be hidden in the high-power jamming signal to fight against the eavesdropping. Thus, based on the joint optimization of power allocation and UAV trajectory, we have the following constraint.

$$\begin{aligned} &h_{u_{in}}^2[n]p_{u_{1n}}[n]\leq h_{u_{in}}^2[n]p_{u_{2n}}[n]\leq ...\leq h_{u_{in}}^2[n]p_{u_{in}}[n] \\ &\leq ...\leq h_{u_{in}}^2[n]p_{u_{Cn}}[n]\leq h_{u_{in}}^2[n]P_{jam}[n], \quad i=1,...,C. \end{aligned} \quad (5)$$

In conventional NOMA systems, u_{in} needs to decode the jamming signal and the messages from u_{Cn} to $u_{(i+1)n}$ before decoding its own, and the signal-to-interference-plus-noise-ratio (SINR) of u_{in} at u_{wn} can be derived as

$$\begin{aligned} \mathrm{SINR}_{u_{wn}}^{u_{in}}[n]=&\frac{h_{u_{wn}}^2[n]p_{u_{in}}[n]}{h_{u_{wn}}^2[n]\sum_{m=1}^{i-1}p_{u_{mn}}[n]+\sigma^2}, \\ &i=2,...,C, \quad w=1,...,i. \end{aligned} \quad (6)$$

When $i=1$, the decoding signal-to-noise ratio (SNR) of u_{1n} can be denoted as $\mathrm{SINR}_{u_{1n}}[n]=h_{u_{1n}}^2[n]p_{u_{1n}}[n]/\sigma^2$. Thus, the transmission rate of u_{in} in the nth time slot can be denoted as

$$R_{u_{in}}[n]=\log_2(1+\min\{\mathrm{SINR}_{u_{wn}}^{u_{in}}[n]\}), i=2,...,C, w=1,...,i. \quad (7)$$

Similarly, when $i=1$, the transmission rate of u_{1n} in the nth time slot can be expressed as

$$R_{u_{1n}}[n]=\log_2\left(1+h_{u_{1n}}^2[n]p_{u_{1n}}[n]/\sigma^2\right). \quad (8)$$

In order to guarantee the SIC, we should satisfy

$$R_{u_{in}}[n]\geq r, n=1,...,N, i=1,...,C, \quad (9)$$

where r is the minimum transmission rate required by users.

In addition, the speed of UAV should be limited, which cannot exceed its maximum of V_{max}. In the nth time slot, we have

$$\|\mathbf{q}[n+1]-\mathbf{q}[n]\|\leq V_{max}\delta_t, n=1,...,N-1, \quad (10)$$

where $V_{max}\delta_t$ denotes the maximum flight distance of the UAV in each time slot. Then, the eavesdropping rate towards u_{in} can be expressed as

$$R_{e\text{–}u_{in}}[n]=\log_2\left(1+\frac{h_e^2[n]p_{u_{in}}[n]}{h_e^2[n]\left(\sum\limits_{j=1,j\neq i}^{C}p_{u_{jn}}[n]+P_{jam}[n]\right)+\sigma^2}\right). \quad (11)$$

From the expression in (11), we can observe that higher P_{jam} leads to lower eavesdropping rate. This is because the eavesdropper does not have the priori knowledge of the legitimate transmission, and it cannot eliminate the artificial jamming. Thus, the security of the network can be guaranteed.

III. Problem Formulation

In this section, the joint power allocation and trajectory optimization problem is formulated. We assume that the C closest users to the UAV are served in each time slot, the set of which can be denoted as $\mathbf{U} = \{\mathcal{U}[n], n = 1, ..., N\}$. As discussed before, increasing P_{jam} can degrade the eavesdropping rate. However, it will also reduce the average transmission rate because of less power allocated to the legitimate users. Thus, we propose the trade-off optimization problem based on the jamming power and the sum rate. By jointly optimizing $\mathbf{P} = \{P_{jam}[n], p_{u_{in}}[n]\}$, UAV trajectory $\mathbf{Q} = \{\mathbf{q}[n]\}$ and user scheduling $\mathbf{U} = \{\mathcal{U}[n], n = 1, ..., N\}$, we can ensure the secure transmission for all users. The optimization problem can be formulated as

$$\max_{\mathbf{P},\mathbf{Q},\mathbf{U}} \ a\frac{1}{N}\sum\nolimits_{n=1}^{N} P_{jam}[n] + (1-a)\frac{1}{N}\sum\nolimits_{n=1}^{N}\sum\nolimits_{i=1}^{C} R_{u_{in}}[n] \quad (12a)$$

$$s.t. \ \ \mathbf{q}[1] = \mathbf{a}, \ \ \mathbf{q}[N] = \mathbf{b}, \quad (12b)$$

$$\|\mathbf{q}[n+1] - \mathbf{q}[n]\| \le V_{max}\delta_t, n = 1, ..., N-1, \quad (12c)$$

$$R_{u_{in}}[n] \ge r, \quad (12d)$$

$$P_{jam}[n] + \sum_{i=1}^{C} p_{u_{in}}[n] \le P_{sum}, n = 1, ..., N, \quad (12e)$$

$$0 \le p_{u_1 n}[n] \le ... \le p_{u_{in}}[n] \le ... \le p_{u_{Cn}}[n] \le P_{jam}[n], \quad (12f)$$

where (12b) illustrates the starting and ending coordinates of the UAV flight. (12c) ensures that the flight speed of UAV should not exceed the maximum speed V_{max}. (12d) sets the minimum rate. (12e) indicates the sum power of the jamming signal and the accessed users in each time slot should be no higher than P_{sum}. (12f) indicates the decoding order, where the jamming signal is first to be decoded, and then the others are decoded according to the distance.

The parameter a in (12a) is to balance between the jamming power and the sum rate within the N time slots, satisfying $0 \le a \le 1$. The jamming power increases as a becomes larger, raising security but decreasing the transmission rate. On the contrary, a smaller a leads to higher transmission rate but less security.

IV. Iterative Solution to the Problem

In this section, we decompose the optimization problem (12) into two subproblems, i.e., power allocation and trajectory optimization. The non-convex constraints in each subproblem are transformed and then solved iteratively.

A. Power Allocation Optimization

With fixed trajectory $\mathbf{Q}$, we have

$$\max_{\mathbf{P}} \ a\frac{1}{N}\sum_{n=1}^{N} P_{jam}[n] + (1-a)\frac{1}{N}\sum_{n=1}^{N}\sum_{i=1}^{C} R_{u_{in}}[n] \quad (13a)$$

$$s.t. \ \ (12d), (12e) \text{ and } (12f).$$

The optimization problem in (13) is non-convex as the objective function (13a) and the constraint (12d) are non-convex. It is difficult to solve directly. Consequently, we introduce the auxiliary variables $t_i[n], i = 1, .., C$, and (13) can be transformed into

$$\max_{\mathbf{P}} \ a\frac{1}{N}\sum_{n=1}^{N} P_{jam}[n] + (1-a)\frac{1}{N}\sum_{n=1}^{N}\log_2\left(\prod_{i=1}^{C} t_i[n]\right) \quad (14a)$$

$$s.t. \ \ 1 + \min\{\text{SINR}_{u_{wn}}^{u_{in}}\}[n] \ge t_i[n], i = 1, ..., C, w = 1, ..., i, \quad (14b)$$

$$t_i[n] \ge r, \text{ and } (12e), \ (12f). \quad (14c)$$

Since the logarithmic function in (14a) is still non-decreasing, it can be converted to maximize the geometric mean as

$$a\frac{1}{N}\sum_{n=1}^{N} P_{jam}[n] + (1-a)\frac{1}{N}\sum_{n=1}^{N}\left(\prod_{i=1}^{C} t_i[n]\right)^{\frac{1}{C}}. \quad (15)$$

Then, according to (6) and (7), (14b) can be rewritten as

$$h_{u_{wn}}^2[n]\sum_{j=1}^{i-1} p_{u_{jn}}[n] + \sigma^2 \le \frac{h_{u_{wn}}^2[n] p_{u_{in}}[n]}{t_i[n] - 1}, i = 1, ..., C. \quad (16)$$

The right side of (16) is non-convex. To deal with it, we adopt Taylor expansion to transform it into a convex one.

we can transform the right side of the inequality in (16) into convex ones by the following proposition.

Proposition 1: The constraint (16) can be approximately transformed into

$$h_{u_{wn}}^2[n]\sum_{j=1}^{i-1} p_{u_{jn}}[n] + \sigma^2 \le \mathcal{L}_1(p_{u_{jn}}[n], \overline{p}_{u_{jn}}[n], t_i[n], \overline{t}_i[n]), \quad (17a)$$

$$\mathcal{L}_1(p_{u_{jn}}[n], \overline{p}_{u_{jn}}[n], t_i[n], \overline{t}_i[n]) = \frac{h_{u_{wn}}^2[n] p_{u_{in}}[n]}{\overline{t}_i[n] - 1} - \frac{h_{u_{wn}}^2[n]\overline{p}_{u_{in}}[n]}{(\overline{t}_i[n] - 1)^2}(t - \overline{t}_i[n]). \quad (17b)$$

Proof: For convenience, we define

$$F_1(p, t) = \frac{h^2 p}{t - 1}, \quad (18)$$

where h is a constant, and $t > 1$. According to Taylor expansion, we have

$$F_1(p, t) \ge F_1(\overline{p}, \overline{t}) + \bigtriangledown_p F_1|_{(\overline{p},\overline{t})}(p - \overline{p}) + \bigtriangledown_t F_1|_{(\overline{p},\overline{t})}(t - \overline{t}) \triangleq \mathcal{L}_1(p, \overline{p}, t, \overline{t}), \quad (19)$$

where

$$\mathcal{L}_1(p, \overline{p}, t, \overline{t}) = \frac{h^2\overline{p}}{\overline{t} - 1} + \frac{h^2}{\overline{t} - 1}(p - \overline{p}) - \frac{h^2\overline{p}}{(\overline{t} - 1)^2}(t - \overline{t}). \quad (20)$$

At this point, (18) can be approximated as convex, and when $p = \overline{p}$ and $t = \overline{t}$, the equality in (19) holds.

Let $p = p_{u_{in}}[n]$, $t = t_i[n]$ and $h^2 = h_{u_{wn}}^2[n]$, and we have

$$h_{u_{wn}}^2[n]\sum_{j=1}^{i-1} p_{u_{jn}}[n] + \sigma^2 \le \frac{h_{u_{wn}}^2[n] p_{u_{in}}[n]}{\overline{t}_i[n] - 1} - \frac{h_{u_{wn}}^2[n]\overline{p}_{u_{in}}[n]}{(\overline{t}_i[n] - 1)^2}(t_i[n] - \overline{t}_i[n]), i = 1, ..., C, \ w = 1, ..., i. \quad (21)$$

Thus, (16) can be approximated as a convex constraint. ■

After the above approximations, all the constraints in (14) become convex. In addition, the geometric mean in (15) can be further converted into a second-order cone programming (SOCP), where the hyperbolic constraint $z^2 \leq xy$ $(x \geq 0, y \geq 0)$ can be changed into $\|[2z, x-y]^\dagger\| \leq x+y$. Accordingly, we transform (14) into a convex (22) at the top of next page. $\mathcal{H} = \lceil \log_2 C \rceil$ is a ceiling function that returns the minimum integer no less than $\log_2 C$.

B. Trajectory Optimization

With given transmit power, the optimization problem should be further written. and **U** should be updated according to the trajectory in each time slot. Since the objective in (12) is non-convex, we transform it by introducing auxiliary variables $\widetilde{t}_i[n]$, and (12) can be rewritten as

$$\max_{\mathbf{Q},\mathbf{U}} \ \frac{1}{N}\sum\nolimits_{n=1}^{N}\sum\nolimits_{i=1}^{C}\widetilde{t}_{in}[n] \tag{23a}$$

$$s.t. \ \ R_{u_{in}}[n] \geq \widetilde{t}_i[n], \tag{23b}$$

$$\widetilde{t}_i[n] \geq r, \text{ and (12b), (12c)}, \tag{23c}$$

The problem (23) is still non-convex due to the non-convex constraint (23b). Thus, let $\gamma = \frac{\rho}{\sigma^2}$, we transform (23b) into

$$\log_2\left(1+\min\left\{\frac{\frac{\gamma p_{u_{in}}[n]}{\|\mathbf{q}[n]-\mathbf{x}_{u_{wn}}\|^2+H^2}}{1+\sum\limits_{j=1}^{i-1}\frac{\gamma p_{u_{jn}}[n]}{\|\mathbf{q}[n]-\mathbf{x}_{u_{wn}}\|^2+H^2}}\right\}\right) \geq \widetilde{t}_i[n]. \tag{24}$$

Then, we introduce the auxiliary variables $z_{u_{wn}}^{u_{in}}[n]$ and $v_{u_{wn}}^{u_{jn}}[n]$, $i=1,...,C$, $w=1,...,i$, and (24) can be approximated as

$$\log_2\left(1+e^{z_{u_{wn}}^{u_{in}}[n]-v_{u_{wn}}^{u_{jn}}[n]}\right) \geq \widetilde{t}_i[n], \tag{25a}$$

$$\frac{\gamma p_{u_{in}}[n]}{H^2+\|\mathbf{q}[n]-\mathbf{x}_{u_{wn}}\|^2} \geq e^{z_{u_{wn}}^{u_{in}}[n]}, \tag{25b}$$

$$1+\sum\nolimits_{j=1}^{i-1}\frac{\gamma p_{u_{jn}}[n]}{H^2+\|\mathbf{q}[n]-\mathbf{x}_{u_{wn}}\|^2} \leq e^{v_{u_{wn}}^{u_{jn}}[n]}. \tag{25c}$$

The inequations of (25a) - (25c) are non-convex. Thus, we introduce Proposition 2 to approximate them.

Proposition 2: Define a function $F_3(z,v)$ as

$$F_3(z,v) = \log_2(1+e^{z-v}), \forall z, v \in \mathbb{R}. \tag{26}$$

The first-order Taylor expansion of $F_3(z,v)$ at the point $(\overline{z},\overline{v})$ can be expressed as

$$\mathcal{F}_3(\overline{z},\overline{v}) = \log_2\left(1+e^{\overline{z}-\overline{v}}\right) + \frac{e^{\overline{z}-\overline{v}}}{\ln 2(1+e^{\overline{z}-\overline{v}})} \times (z-v-\overline{z}+\overline{v}). \tag{27}$$

Thus, $F_3(z,v)$ can be replaced by $\mathcal{F}_3(\overline{z},\overline{v})$.

Proof: The Hessian matrix of $F_3(z,v)$ can be denoted as

$$\bigtriangledown^2 F_3(z,v) = \frac{e^{z-v}}{(1+e^{z-v})^2\ln 2}\begin{bmatrix}1 & -1\\ -1 & 1\end{bmatrix} \succ \mathbf{0}. \tag{28}$$

The Hessian matrix of $F_3(z,v)$ is semidefinite, and thus (28) is convex for z and v. According to the Taylor expansion, $F_3(z,v)$ satisfies the following expression with the given $\overline{z}$ and $\overline{v}$ as

$$F_3(z,v) \geq F_3(\overline{z},\overline{v}) = \log_2(1+e^{\overline{z}-\overline{v}}) + \frac{e^{\overline{z}-\overline{v}}}{(1+e^{\overline{z}-\overline{v}})\ln 2} \times (z-\overline{z}-v+\overline{v}), \tag{29}$$

where the equality holds when $z=\overline{z}$ and $v=\overline{v}$. Then, $F_3(z,v)$ can be replaced by (27). ■

Let $z = z_{u_{wn}}^{u_{in}}[n]$ and $v = v_{u_{wn}}^{u_{jn}}[n]$, (25a) can be written as

$$\log_2\left(1+e^{\overline{z}_{u_{wn}}^{u_{in}}[n]-\overline{v}_{u_{wn}}^{u_{jn}}[n]}\right) + \frac{e^{\overline{z}_{u_{wn}}^{u_{in}}[n]-\overline{v}_{u_{wn}}^{u_{jn}}[n]}}{(1+e^{\overline{z}_{u_{wn}}^{u_{in}}[n]-\overline{v}_{u_{wn}}^{u_{jn}}[n]})\ln 2} \times (z_{u_{wn}}^{u_{in}}[n]-\overline{z}_{u_{wn}}^{u_{in}}[n]-z_{u_{wn}}^{u_{in}}[n]+\overline{v}_{u_{wn}}^{u_{jn}}[n]) \geq \widetilde{t}_i[n]. \tag{30}$$

The constraint (25b) can be rewritten as

$$\frac{H^2}{\gamma p_{u_{in}}[n]} + \frac{\|\mathbf{q}[n]-\mathbf{x}_{u_{wn}}\|^2}{\gamma p_{u_{in}}[n]} \leq e^{-z_{u_{wn}}^{u_{in}}[n]}, \tag{31}$$

which can be proved as convex in the following proposition.

Proposition 3: Define a function $g(x,y)$ as

$$g(x,y) = \|x-b\|^2/y, \forall x, b \in \mathbb{R}, y > 0, \tag{32}$$

where b is a constant.

Proof: The Hessian matrix of $g(x,y)$ can be denoted as

$$\bigtriangledown^2 g(x,y) = \frac{2}{y^2}\begin{bmatrix}\sqrt{y}\mathbf{I}_m \\ \frac{-x}{\sqrt{y}}^T\end{bmatrix}\begin{bmatrix}\sqrt{y}\mathbf{I}_m & \frac{-x}{\sqrt{y}}\end{bmatrix} \succ \mathbf{0}, \tag{33}$$

where $\mathbf{I}_m$ is the identity matrix of order m. The Hessian matrix of $g(x,y)$ is always larger than **0**, and thus it is a convex function. Thus, the function $\frac{\|\mathbf{q}[n]-\mathbf{x}_{u_{wn}}\|^2}{\gamma p_{u_{in}}[n]}$ is a convex one with respect to $\mathbf{q}[n]$ and $p_{u_{in}}[n]$. Moreover, the function $\frac{H^2}{\gamma p_{u_{in}}[n]}$ is convex with respect to $p_{u_{in}}[n]$. Since the non-negative weighted sum of convex functions is still convex, we can conclude that the function $\frac{H^2}{\gamma p_{u_{in}}[n]} + \frac{\|\mathbf{q}[n]-\mathbf{x}_{u_{wn}}\|^2}{\gamma p_{u_{in}}[n]}$ is convex with respect to $\mathbf{q}[n]$ and $p_{u_{in}}[n]$. Thus, the left side of (31) is convex. ■

To satisfy the constraints of SOCP, the right side of (31) should be concave, which can be transformed by Taylor expansion as

$$M(z) \geq \mathcal{M}(z,\overline{z}) = M(\overline{z}) + \bigtriangledown M(\overline{z})(z-\overline{z}) = e^{-\overline{z}}(1-z+\overline{z}). \tag{34}$$

Thus, we can approximate (31) as

$$\frac{H^2}{\gamma p_{u_{in}}[n]} + \frac{\|\mathbf{q}[n]-\mathbf{x}_{u_{wn}}\|^2}{\gamma p_{u_{in}}[n]} \leq e^{-\overline{z}_{u_{wn}}^{u_{in}}[n]}\left(1-z_{u_{wn}}^{u_{in}}[n]+\overline{z}_{u_{wn}}^{u_{in}}[n]\right). \tag{35}$$

For the constraint (25c), two auxiliary variables $s_{u_{wn}}[n]$ and $y_{u_{jn}}^{u_{in}}[n]$ are introduced, and (25c) can be rewritten as

$$s_{u_{wn}}[n] \leq H^2 + \|\mathbf{q}[n]-\mathbf{x}_{u_{wn}}\|^2, w=1,...,i, i=1,...,C, \tag{36a}$$

$$\frac{\gamma p_{u_{jn}}[n]}{s_{u_{wn}}[n]} \leq y_{u_{wn}}^{u_{jn}}[n], j=1,...,C-1, \tag{36b}$$

$$1+\sum\nolimits_{j=1}^{i-1} y_{u_{wn}}^{u_{jn}} \leq e^{v_{u_{wn}}^{u_{jn}}[n]}. \tag{36c}$$

However, the above constraints are still non-convex, which

$$\max_{\mathbf{P},t_m} \ a\frac{1}{N}\sum\nolimits_{n=1}^{N} P_{jam}[n] + (1-a)\frac{1}{N}\sum\nolimits_{n=1}^{N} t_1^0[n] \tag{22a}$$

$$s.t. \ \ \|[2t_m^{\mathcal{H}-1}[n], (t_{2m-1}[n] - t_{2m}[n])]\| \le t_{2m-1}[n] + t_{2m}[n], \ m = 1, 2, ...2^{\mathcal{H}-1}, \tag{22b}$$

$$\|[2t_m^{\mathcal{H}-2}[n], (t_{2m-1}^{\mathcal{H}-1}[n] - t_{2m}^{\mathcal{H}-1}[n])]\| \le t_{2m-1}^{\mathcal{H}-1}[n] + t_{2m}^{\mathcal{H}-1}[n], \ m = 1, 2, ...2^{\mathcal{H}-2}, \tag{22c}$$

$$.....$$

$$\|[2t_1^0[n], (t_1^1[n] - t_2^1[n])]\| \le t_1^1[n] + t_2^1[n], \ m = 1, \tag{22d}$$

$$t_m^{\mathcal{H}-1}[n] \ge 2^r, \ m = 1, 2, ...2^{\mathcal{H}-1}, \text{ and (12e), (12f), (21).} \tag{22e}$$

should be further formulated.

For (36a) and (36b), we use the first order Taylor expansion. Two functions are defined as

$$F_4(\mathbf{q}[n]) = \|\mathbf{q}[n] - \mathbf{x}_{u_{wn}}\|^2, \tag{37}$$

$$F_5(u_{wn}[n]) = \frac{1}{s_{u_{wn}}[n]}, \tag{38}$$

where $w = 1, ..., i$. The approximate first-order Taylor expansion of $F_4(\mathbf{q}[n])$ and $F_5(s_{u_{wn}})$ at $(\overline{\mathbf{q}}[n])$ and $(\overline{s}_{u_{wn}}[n])$ can be written as

$$\begin{aligned}\mathcal{F}_4(\overline{\mathbf{q}}[n],\mathbf{q}[n]) &= F_4(\overline{\mathbf{q}}[n]) + \bigtriangledown F_4(\overline{\mathbf{q}}[n])(\mathbf{q}[n] - \overline{\mathbf{q}}[n]) \\ &= \|\overline{\mathbf{q}}[n] - \mathbf{x}_{u_{wn}}\|^2 + 2(\overline{\mathbf{q}}[n] - \mathbf{x}_{u_{wn}})^T(\mathbf{q}[n] - \overline{\mathbf{q}}[n]),\end{aligned} \tag{39}$$

$$\begin{aligned}\mathcal{F}_5(\overline{s}_{u_{wn}}[n], s_{u_{wn}}) &= F_5(\overline{s}_{u_{wn}}[n]) + \bigtriangledown F_5(\overline{s}_{u_{wn}}[n])(s_{u_{wn}} - \overline{s}_{u_{wn}}[n]) \\ &= \frac{1}{\overline{s}_{u_{wn}}[n]} - \frac{1}{\overline{s}_{u_{wn}}^2[n]}(s_{u_{wn}} - \overline{s}_{u_{wn}}[n]).\end{aligned} \tag{40}$$

Then, (36a) and (36b) can be rewritten as

$$s_{u_{wn}}[n] \le H^2 + \|\overline{\mathbf{q}}[n] - \mathbf{x}_{u_{wn}}\|^2 + 2(\overline{\mathbf{q}}[n] - \mathbf{x}_{u_{wn}})^T(\mathbf{q}[n] - \overline{\mathbf{q}}[n]), \tag{41a}$$

$$\frac{\gamma p_{u_{jn}}[n]}{\overline{s}_{u_{wn}}[n]} - \frac{\gamma p_{u_{jn}}[n]}{\overline{s}_{u_{wn}}^2[n]}(s_{u_{wn}}[n] - \overline{s}_{u_{wn}}[n]) \le y_{u_{wn}}^{u_{jn}}[n]. \tag{41b}$$

Similarly, we can apply Proposition 4 to obtain an approximation of (36c) as

$$1 + \sum\nolimits_{j=1}^{i-1} y_{u_{wn}}^{u_{jn}}[n] \le e^{\overline{v}_{u_{in}}[n]}(v_{u_{wn}}^{u_{jn}}[n] - \overline{v}_{u_{wn}}^{u_{jn}}[n] + 1). \tag{42}$$

Since (25a), (25b) and (25c) have been converted into convex ones, the optimization problem (12) is transformed into (43), which can be solved via CVX.

$$\begin{aligned}\max_{\mathbf{Q},\mathbf{U}} \ & \frac{1}{N}\sum\nolimits_{n=1}^{N}\sum\nolimits_{i=1}^{C} \widetilde{t}_{in}[n] \\ s.t. \ & \text{(12b), (12c), (23c), (30). (35),} \\ & \text{(41a), (41b), (42).}\end{aligned} \tag{43}$$

C. Proposed Algorithm

Since (22) and (43) have been proved to be SOCP, an iterative algorithm is proposed to solve the problem in (12) as Algorithm 1, where $\mathbf{Q} = \{\mathbf{q}[n]\}$ and $\mathbf{P} = \{P_{jam}[n], p_{u_{in}}[n]\}$, $n = 1, ..., N, i = 1, ..., C$. $\mathbf{Q}^t$ and $\mathbf{P}^t$ represent the UAV's location and transmit power in each iteration t, respectively.

Algorithm 1 Iterative algorithm for (12)

1: Initialization: Set the initial values of $\{\mathbf{Q}^0, \mathbf{P}^0\}$. Set the index of iteration $t = 0$. $\mathbf{U}^0$ is obtained from $\mathbf{Q}^0$.
2: **repeat**
3: Solve the problem of (22) with the given $\mathbf{Q}^t$ and the new value of $\mathbf{P}^{t+1}$ can be obtained.
4: Calculate the the solution to (43) with $\mathbf{P}^{t+1}$ and the new value of $\mathbf{Q}^{t+1}$. can be obtained.
5: Update the current value of the elements in $\mathbf{U}^t = \{\mathcal{U}[n], n = 1, ..., N\}$.
6: Update: $t = t + 1$.
7: **until** The increase of the optimal value is below a predetermined threshold.

V. Simulation Results and Discussion

In this section, simulation results are presented to evaluate the performance of the proposed scheme. Assume that the total number of users $K = 10$, and they are randomly distributed in a rectangular area of 1000×120 m^2. The initial location of UAV is $\mathbf{a} = (0, 0)$ and its destination is $\mathbf{b} = (1000, 0)$ in meters. The altitude of UAV is set as $H = 100$ m. During the flight, the closest three users can be served by UAV in each time slot, i.e., $C = 3$. Furthermore, $\rho = 10^{-4}$, and the noise power $\sigma^2 = -110$ dBm. The maximum speed is $V_{max} = 30$ m/s, and the sum transmit power is set to 1 W. The rate threshold is set to 0.5 bit/s/Hz. The optimized UAV trajectory with the topology of 10 users and an eavesdropper is presented in Fig. 1. The sum time slots is set to $N = 300$ and each time slot is $\delta_t = 0.3$ s. The eavesdropper is located at $(450, 10)$ in meters. Thus, all the users are under the risk of being eavesdropped. The dense flight trajectory indicates that the UAV flies slow to satisfy the requirement of the densely located users, and on the contrary, it flies fast when the users are distributed sparsely.

For different values of a, the sum transmission rate and eavesdropping rate are shown in Fig. 2. We set the weight of the jamming power to $a = 0.1$, 0.3, 0.5, 0.7 and 0.9, respectively. From the results, we can observe that both the sum transmission rate and eavesdropping rate decrease with the increase of a, because the jamming power increases as the weight a grows. Accordingly, less transmit power is allocated to each user, which degrades the transmission performance.

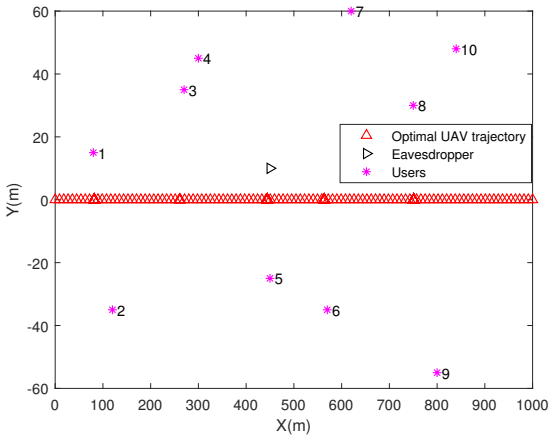

Fig. 1. The optimized UAV trajectory with 10 users in the proposed scheme. $H = 100$ m, $N = 300$, $\delta_t = 0.3$ s and $a = 0.5$.

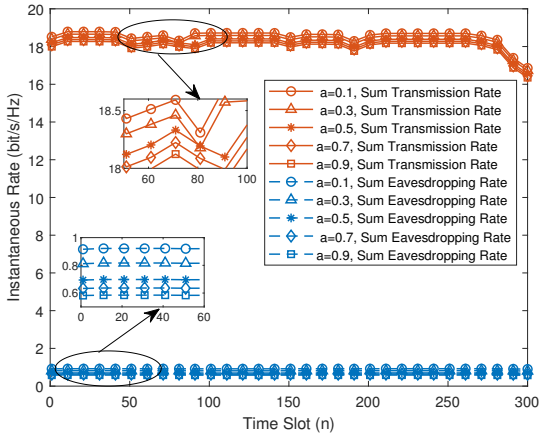

Fig. 2. Instantaneous rate comparison of the proposed scheme with different values of a. $H = 100$ m, $N = 300$, and $\delta_t = 0.3$ s.

In addition, the eavesdropping rate can be suppressed to less than 1 bit/s/Hz, and decreases with the growth of a in each time slot.

The eavesdropping rate and the secrecy rate of the proposed scheme and the scheme without jamming are compared in Fig. 3. We can see that the eavesdropping rate of the proposed scheme is much lower than that of the scheme without jamming. Thus, the secrecy rate of the proposed jamming scheme is higher than that of the scheme without jamming. This is because the eavesdropping rate gradually decreases as the jamming power increases in the denominator of (11). We can conclude that the eavesdropping rate can be effectively suppressed via artificial jamming, and thus the security of the network can be guaranteed.

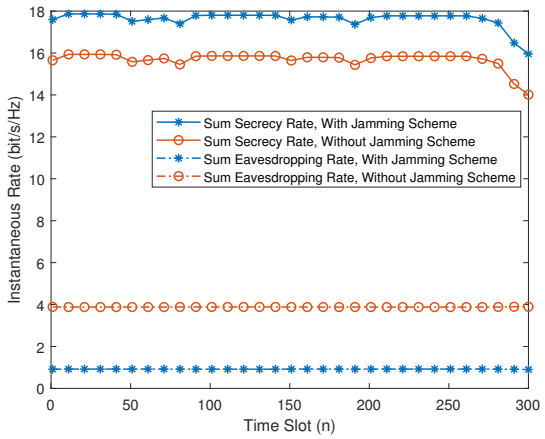

Fig. 3. Comparison of eavesdropping rate and secrecy rate in the proposed jamming scheme and the scheme without jamming. $H = 100$ m, $N = 300$, $\delta_t = 0.3$ s and $a = 0.5$.

REFERENCES

[1] S. Hayat, E. Yanmaz, and R. Muzaffar, "Survey on unmanned aerial vehicle networks for civil applications: A communications viewpoint," *IEEE Commun. Surveys Tuts.*, vol. 18, no. 4, pp. 2624–2661, 4th Quart. 2016.

[2] Y. Zeng, R. Zhang, and T. J. Lim, "Wireless communications with unmanned aerial vehicles: opportunities and challenges," *IEEE Commun. Mag.*, vol. 54, no. 5, pp. 36–42, May. 2016.

[3] J. Lyu, Y. Zeng, R. Zhang, and T. J. Lim, "Placement optimization of UAV-mounted mobile base stations," *IEEE Commun. Lett.*, vol. 21, no. 3, pp. 604–607, Mar. 2017.

[4] H. Wu, X. Tao, N. Zhang, and X. Shen, "Cooperative UAV cluster-assisted terrestrial cellular networks for ubiquitous coverage," *IEEE J. Select. Areas Commun.*, vol. 36, no. 9, pp. 2045–2058, Sept. 2018.

[5] Z. Ding, X. Lei, G. K. Karagiannidis, R. Schober, J. Yuan, and V. K. Bhargava, "A survey on non-orthogonal multiple access for 5G networks: Research challenges and future trends," *IEEE J. Select. Areas Commun.*, vol. 35, no. 10, pp. 2181–2195, Oct. 2017.

[6] Z. Chen, Z. Ding, X. Dai, and G. K. Karagiannidis, "On the application of quasi-degradation to MISO-NOMA downlink," *IEEE Trans. Signal Process.*, vol. 64, no. 23, pp. 6174–6189, Dec. 2016.

[7] Y. Wu, L. P. Qian, H. Mao, X. Yang, H. Zhou, and X. Shen, "Optimal power allocation and scheduling for non-orthogonal multiple access relay-assisted networks," *IEEE Trans. Mobile Comput.*, vol. 17, no. 11, pp. 2591–2606, Nov. 2018.

[8] Y. Liu, Z. Qin, Y. Cai, Y. Gao, G. Y. Li, and A. Nallanathan, "UAV communications based on non-orthogonal multiple access," *IEEE Wireless Commun.*, vol. 26, no. 1, pp. 52–57, Feb. 2019.

[9] N. Zhao, Y. Li, S. Zhang, Y. Chen, W. Lu, J. Wang, and X. Wang, "Security enhancement for NOMA-UAV networks," *IEEE Trans. Veh. Technol.*, vol. 69, no. 4, pp. 3994–4005, Apr. 2020.

[10] N. Zhao, X. Pang, Z. Li, Y. Chen, F. Li, Z. Ding, and M. Alouini, "Joint trajectory and precoding optimization for UAV-assisted NOMA networks," *IEEE Trans. Commun.*, vol. 67, no. 5, pp. 3723–3735, May. 2019.

[11] I. Budhiraja, N. Kumar, S. Tyagi, and S. Tanwar, "Energy consumption minimization scheme for NOMA-based mobile edge computation networks underlaying UAV," *IEEE Syst. J.*, to appear.

[12] Q. Wang, Z. Chen, W. Mei, and J. Fang, "Improving physical layer security using UAV-enabled mobile relaying," *IEEE Wireless Commun. Lett.*, vol. 6, no. 3, pp. 310–313, Jun. 2017.

[13] F. Cheng, G. Gui, N. Zhao, Y. Chen, J. Tang, and H. Sari, "UAV-relaying-assisted secure transmission with caching," *IEEE Trans. Commun.*, vol. 67, no. 5, pp. 3140–3153, May. 2019.

[14] Y. Zou, J. Zhu, X. Wang, and L. Hanzo, "A survey on wireless security: Technical challenges, recent advances, and future trends," *Proc. IEEE*, vol. 104, no. 9, pp. 1727–1765, Sept. 2016.

[15] H.-M. Wang and X. Zhang, "UAV secure downlink NOMA transmissions: A secure users oriented perspective," *IEEE Trans. Commun.*, vol. 68, no. 9, pp. 5732–5746, Sept. 2020.

[16] X. Sun, W. Yang, and Y. Cai, "Secure communication in NOMA-assisted millimeter-wave SWIPT UAV networks," *IEEE Internet Things J.*, vol. 7, no. 3, pp. 1884–1897, Mar. 2020.